Accepted Manuscript

Determination of Uric Acid in Synthetic Urine by Using Electrochemical Surface Oxidation Enhanced Raman Scattering

Sheila Hernandez, Juan V. Perales-Rondon, Aranzazu Heras, Alvaro Colina

PII: S0003-2670(19)30881-5

DOI: https://doi.org/10.1016/j.aca.2019.07.057

Reference: ACA 236964

To appear in: *Analytica Chimica Acta*

Received Date: 18 June 2019

Revised Date: 25 July 2019

Accepted Date: 27 July 2019

Please cite this article as: S. Hernandez, J.V. Perales-Rondon, A. Heras, A. Colina, Determination of Uric Acid in Synthetic Urine by Using Electrochemical Surface Oxidation Enhanced Raman Scattering, *Analytica Chimica Acta*, https://doi.org/10.1016/j.aca.2019.07.057.

Determination of Uric Acid in Synthetic Urine by Using Electrochemical Surface Oxidation Enhanced Raman Scattering

Sheila Hernandez, Juan V. Perales-Rondon*, Aranzazu Heras, Alvaro Colina*.

Department of Chemistry, Universidad de Burgos, Pza. Misael Bañuelos s/n, E-09001 Burgos, Spain

Email address: acolina@ubu.es (Alvaro Colina), jvperales@ubu.es (Juan V. Perales-Rondon)

Abstract

In this work, a new and easy methodology to determine uric acid in relevant samples using Raman spectroelectrochemistry is presented. The spectroelectrochemistry experiment is based on the in-situ formation of a suitable substrate that enables the enhancement of the Raman signal of an analyte during the oxidation stage of a silver electrode. This phenomenon is known as electrochemical surface oxidation enhanced Raman scattering (EC-SOERS) and has proved to be useful in quantitative analysis using disposable screen printed electrodes. The successful combination of EC-SOERS with PARAFAC analysis allows the determination of uric acid in a relevant complex sample avoiding the use of standard addition method and without using a baseline correction, which simplifies the application of such methodology in routine analysis.

Keywords

Spectroelectrochemistry; Electrochemistry; Raman; EC-SOERS.

1. Introduction

Raman spectroscopy is a powerful technique because it provides specific structural information that can be used for qualitative and quantitative analysis in very different research fields [1,2]. However, despite the important information provided by Raman spectroscopy, its development is limited because of the weakness of the intensity of the Raman signal. To overcome this limitation, surface enhanced Raman scattering (SERS) emerged more than 40 years ago [3] and, since then, numerous scientists of all disciplines have used it for diverse purposes [4–6]. SERS is associated with the amplification, by several orders of magnitude, of Raman signals of analytes located at or very close to metallic nanostructures, which should have plasmonic properties. SERS phenomenon can be explained by the contribution of two mechanisms: the electromagnetic enhancement [7] which is largely due to the amplification of the local electromagnetic (EM) fields owing to the excitation of surface-plasmon resonance [8]; and the chemical enhancement [9,10], which involves charge transfer mechanisms, where a resonance between the excitation wavelength with the metal-molecule charge transfer electronic states is taking place [1]. The appropriate combination of them will determine the total Raman enhancement achieved in a SERS experiment [2].

To obtain a good SERS signal, the preparation of a suitable metal substrate is a mandatory step [11]. One of the most popular and easy methods to achieve this goal consists of the electrochemical roughening of a metal electrode until obtaining a reproducible plasmonic surface. In this sense, the combination of electrochemical methods with spectroscopic techniques, so-called spectroelectrochemistry (SEC), allows taking advantage of the potentialities of these two techniques, promoting a synergistic effect. In particular, electrochemistry allows controlling the electrode potential as well

as the roughness of the metal substrate, while obtaining simultaneously a huge amount of structural information provided by the enhanced Raman signal measured during the time-resolved Raman-SEC (TR-Raman-SEC) experiment. Therefore, the combination of TR-Raman-SEC with the higher sensitivity achieved with SERS, in the technique so-called electrochemical-SERS (EC-SERS) [12], has emerged as a very powerful SEC technique with wide applications in interfacial electrochemistry [13,14], materials characterization [1,4,15], and quantitative analysis [16–19], among others. In fact, in the last years EC-SERS has been deeply developed for routine analysis [18,20,21].

One of the limitations of EC-SERS in quantitative analysis is the lack of reproducibility in the preparation of the SERS substrate, which results in a huge dispersion of the Raman signal [22–25]. Recently a new and unexpected phenomenon parallel to EC-SERS has been discovered. This implies the enhancement of the Raman signal during the electrochemical oxidation of a silver electrode [26]. The phenomenon has been called electrochemical surface oxidation enhanced Raman scattering (EC-SOERS) and has proven to be a reproducible and reliable method to carry out quantitative analysis. The reason behind these special analytical features lies in: (1) the preparation of substrates by oxidation of the silver electrode, which is carried out simultaneously with the measurement of the Raman signal, obtaining a high reproducibility and (2) as a result of this *in-situ* preparation, Raman signal is obtained with low dispersion (variability in the Raman band) at the oxidation stage of the silver electrode.

Hence, in the present work it is proposed the use of EC-SOERS to determine uric acid (UA) in relevant samples (synthetic urine). Although there are numerous techniques to determine uric acid, such as colorimetric enzymatic assays [27–30], liquid chromatography [30–32] or even SERS [21] or EC-SERS [19]. These techniques

present some disadvantages, such as a high cost of materials, an outstanding expertise of the operator as well as long experimental sessions required in the determination. Therefore, EC-SOERS emerges as a fast, easy-to-use, cheap and feasible alternative method to determine UA in relevant samples with high accuracy and reproducibility [17,26], using for that purpose disposable screen printed electrodes (SPE).

Recently, some works assess the UA determination using EC-SERS with very promising results [19]. However, we propose to determine UA in synthetic urine samples using a simpler and easier methodology. EC-SOERS is an alternative to EC-SERS. Nevertheless, EC-SOERS presents some clear advantages over EC-SERS that can be described as follow:

(1) The typical process used in EC-SERS involves the preparation of the substrate (usually, metal nanoparticles with plasmonic properties) which should be synthesized and cleaned in advance. After that, a drop-casting (or another deposition method) should be applied in order to deposit the nanoparticles in the surface of the substrate. All these steps are avoided in an EC-SOERS experiment.

(2) Compared with a typical EC-SERS experiment found in literature, in our approach time-resolved experiments are performed. Therefore, different physical-chemical processes that affect the measurement could be avoided with EC-SOERS.

Preparation of the SERS substrate can be not only time consuming, but also the expertise of the operator must be high enough to carry out all the measurement process at a whole. Compared with EC-SERS, the whole methodology of EC-SOERS is easier, faster and with good analytical figures of merit to be used with analytical purposes.

Uric acid has been determined in urine in very wide ranges of concentration, from 50 nM to 3.6 mM, using very different analytical techniques [32–35]. Particularly, using

EC-SERS, UA has been determined in a range from 0.1 mM to 1 mM [19]. Concentration of UA in human urine depends on the sex and age of the individual, being in the range from 0.12 mM to 0.5 mM [34]. For the application of this technique in relevant samples is mandatory to minimize the matrix effect. Although different approaches have been used to solve this problem, the most conventional way has consisted of the separation of the components of the sample in advance, which allows measuring the analyte without interferences. Nonetheless, these methodologies involve using complex and often expensive instrumentation, in addition to the time consumed in the preparation of the sample and the separation step. Among them, it can be highlighted the chromatographic [36–38] and microfluidic methods [39–41], with wide application in the clinical, pharmaceutical and quality control standard methods. Another possibility implies using the method of standard addition, which allows the minimization of the matrix influence by adding to each calibration sample a constant amount of the sample. In this way, the effect of the different components and its interaction with the analyte remains constant, and the quantification could be carried out with high accuracy [24,42,43]. In this work, EC-SOERS is used to avoid the use of a standard addition calibration, minimizing the experimental time respect to other analytical techniques, as well as diminishing the sources of error because of the simplification in the steps (avoiding separation procedures) employed in the whole analysis protocol.

Finally, and no less important, because of the trilinearity of the data obtained by EC-SOERS, a chemometric method such as parallel factor analysis (PARAFAC) can be used [44–47]. PARAFAC is a useful mathematical tool that allows the separation of different contributions present in the sample [48] such as response of the analyte and matrix effect. Particularly, SEC signals have been successfully used with PARAFAC

because of the trilinear character of the spectroscopic signal [26,45,46]. Moreover, in this work we demonstrate that PARAFAC can be used to avoid baseline corrections, which is a great advantage because it reduces the sources of error that depends on the mathematical method used for fitting the baseline. Hence, in this work, EC-SOERS combined with PARAFAC analysis is presented as an outstanding technique for determination of analytes in complex relevant samples, with high accuracy and good reproducibility.

2. Experimental section

2.1 Reagents and Materials

Uric acid (UA, 99+%, reagent, ACROS Organics), perchloric acid ($HClO_4$, 60 %, reagent, Sigma-Aldrich), potassium chloride (KCl, 99+%, reagent, ACROS Organics) and surine™ (synthetic urine, Sigma-Aldrich), were used. All solutions were prepared using ultrapure water obtained from a Millipore DirectQ purification system provided by Millipore (18.2 MΩ cm resistivity at 25 °C).

2.2 Instrumentation

Raman spectroelectrochemistry. In situ time-resolved Raman spectroelectrochemistry (TR-Raman-SEC) was performed by using a customized SPELEC RAMAN instrument (Metrohm-DropSens), which integrates a laser source of 785 nm. Laser power in all experiments was 80 mW (254 $W \cdot cm^{-2}$). This instrument was connected to a bifurcated reflection probe (DRP-RAMANPROBE, Metrohm-DropSens). A Raman spectroelectrochemical cell especially designed for screen-printed electrodes was employed. DropView SPELEC software (Metrohm-DropSens) was used to control the instrument, which allows us to acquire real-time and synchronized spectroelectrochemical data in a simple way.

Silver screen-printed electrodes (Ag-SPE, DRP-C013, DropSens) were used for all the experiments. These electrodes consist of a flat ceramic card on which a three-electrode system comprising the electrochemical cell is screen-printed. The working silver electrode is circular with a diameter of 1.6 mm, the auxiliary electrode is made of carbon and a silver paint acts as a pseudoreference.

2.3 Time-resolved Raman spectroelectrochemistry experiments

EC-SOERS is obtained during the time-resolved spectroelectrohemical experiment by performing an oxidation-reduction cycle (ORC). Raman spectra were collected with an integration time of 1 s, simultaneously with the electrochemical data, during an ORC. In all the experiments, cyclic voltammetry was carried out between the vertex potentials -0.40 V and +0.40 V, starting at -0.025 V in the anodic direction. The scan rate was 0.02 $V \cdot s^{-1}$. All the spectroelectrochemistry experiments, including synthetic urine samples, were carried out using the same electrolytic medium, containing 0.1 M $HClO_4$ + $5 \cdot 10^{-3}$ M KCl. Before the analytical measurement, a pretreatment to the electrode is performed by cycling twice the potential under the above conditions, but in absence of UA, to improve the reproducibility of the method. Therefore, the time employed for the analysis of each sample is 240 s, approximately, including the change of sample. Each sample was measured in a different silver-SPE. This fact together with the results presented below demonstrates the good reproducibility achieved in EC-SOERS for detection of UA.

2.4 PARAFAC analysis

Matlab R2016b was used to carry out the PARAFAC analysis, using the N-way toolbox, version 3.0, developed by Rasmus Bro [49].

3. Results and discussion

3.1 Spectroscopic and spectroelectrochemistry characterization of uric acid

Before performing the spectroelectrochemical (SEC) experiment, the first step was to evaluate the Raman spectrum of UA in a solid sample and during the EC-SOERS experiment in solution, in order to demonstrate that the signal registered in such experiment belonged unequivocally to the UA molecule. The spectrum for the solid sample was registered and compared with the 150 µM UA spectrum during the EC-SOERS in 0.1 M $HClO_4$ + $5 \cdot 10^{-3}$ M KCl electrolytic medium ($HClO_4$/KCl).

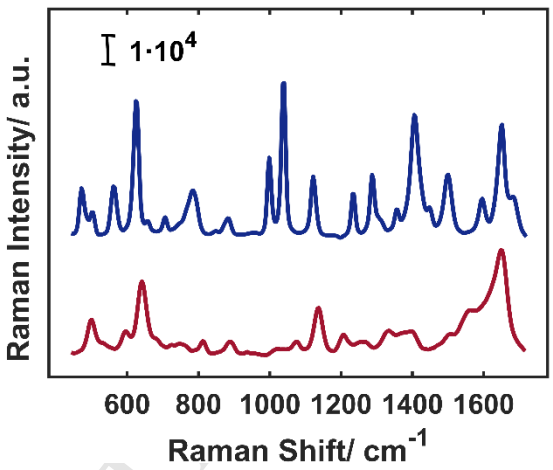

Figure 1. UA Raman spectrum for the solid (blue curve) and 150 µM UA Raman spectrum in $HClO_4$/KCl electrolytic medium at a specific potential during an EC-SOERS experiment (red curve). For a better comparison between the two spectra the intensity of UA Raman spectrum during EC-SOERS experiment (red curve) was amplified 5 times.

As can be observed in Figure 1, there are some differences between the two spectra. Some of the Raman signals found in the solid sample disappeared in the EC-SOERS spectrum. This could be associated with the molecule orientation [50,51] and with the interaction with the EC-SOERS substrate. It is possible that in the SEC experiment, UA

is taking a specific orientation depending on the polarization of the electrode [12]. On the other hand, in the SEC experiment, some of the Raman signals tend to become wider, and also suffer a Raman shift displacement, mainly due to the interaction of the molecule with substrate and electrolytic solution as is well-known from earlier studies [50,51]. Based on the comparison between the spectra in Figure 1, it can be concluded that the spectrum taken in the EC-SOERS experiment corresponds to UA. Bands assignments are shown in Table S1, which are in good agreement with those previously reported in literature [19,21].

3.2 EC-SOERS experiment of uric acid

During the EC-SOERS experiment, Raman spectra of UA were registered with an integration time of 1 s and the potential window was fixed between -0.40 V to +0.40 V. Figure 2 displays the evolution of the Raman intensity of one of the main peak of UA (641 cm^{-1}, which correspond to the ring breathing [19,21], Table S1), respect to the applied potential. This type of representation has been denoted as voltaRamangram in previous works [26,52] for simplification of the terminology. In Figure 2, the Raman signal only appears at anodic potentials, when the silver electrode is being oxidized, but not the studied molecule. This behavior has been previously reported as a new unexpected phenomenon so-called EC-SOERS, as was aforementioned in the introduction section. In this process, the enhancement of Raman signal is occurring probably due to the formation of Ag^{+}/AgCl or Ag/AgCl nanostructures on the electrode surface that interact with the molecule, which is combined with the electrochemical adsorption of the molecule because of the electrode polarization [26,52]. This effect depends strongly on the potential and on the electrolytic conditions, but it provides a good and reproducible enhancement of the Raman signal, being especially useful for

analytical applications. Additionally, in Figure 2 (blue line) can be distinguished that the Raman signal exhibits a maximum at +0.225 V in the cathodic direction (cd), inset in Figure 2, which displays the Raman spectrum (between 550 and 700 cm^{-1}) measured at different potentials until reaching the maximum at +0.225 V in the cathodic direction.

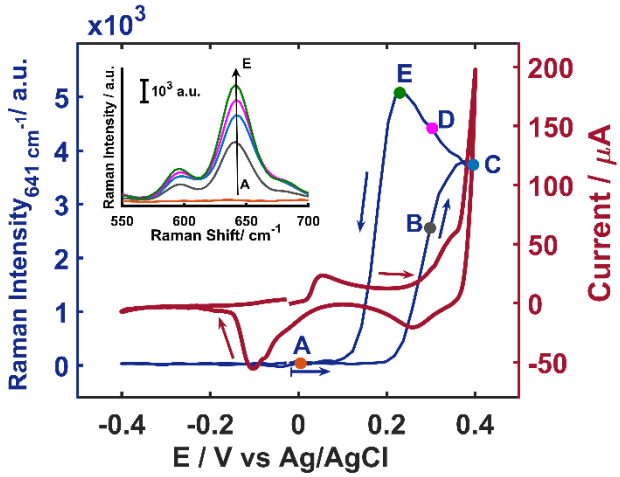

Figure 2. CV (red) of 150 µM UA in $HClO_4$/KCl between the vertex potential of + 0.40 V and - 0.40 V, CV starts at -0.025 V in anodic direction (ad). In blue is shown the VoltaRamangram of UA at 641 cm^{-1}. The inset shows the evolution of Raman spectra (between 550 and 700 cm^{-1}) at different anodic potentials in increasing order, each spectrum correspond to A-E point in the VoltaRamangram.

3.3 Quantitative determination of uric acid in aqueous solution using EC-SOERS

There are a number of works that study the influence of the electrolytic medium and the experimental conditions employed during the surface roughening of a silver electrode for EC-SERS and EC-SOERS. Particularly, a very recent publication has demonstrated the influence of the chloride concentration and pH in the modulation of the EC-SOERS signal [52], with these two parameters being fundamental to obtain a good enhancement

of the signal. In this work, the specific conditions in which the experiments were conducted ($HClO_4$/KCl), allowed us to have a reproducible EC-SOERS signal for UA determination.

Raman response was used, in a first step, to perform a univariate calibration with different concentration of UA in a 0.1 M $HClO_4$ and $5 \cdot 10^{-3}$ M KCl. To carry out the calibration curve, the intensity of the peak at 641 cm^{-1}, at +0.225 V in the cathodic direction was plotted with the UA concentration in a range between 40 and 170 µM. A good linear correlation is obtained evidenced in the R^2 value of 0.99 and the low data dispersion can be observed in Figure 3. With this calibration curve, a test sample was determined with relative error of 4.2 %, which represents a good accuracy. It is noteworthy, the good reproducibility of the employed method (4.4 %RSD), which is not easy to obtain in quantitative Raman. The limit of detection for the univariate calibration was 12.4 µM. The results presented here clearly demonstrate the usefulness of EC-SOERS as a suitable technique for quantitative analysis with high reproducibility. Additionally, if this technique is combined with the use of disposable SPE, the methodology emerges as a good alternative to regular EC-SERS experiments [18,19] to carry out quantitative analysis. Moreover, it is possible to achieve a better reproducibility and less time-consuming experiments, because the nanoparticles preparation and electrode modification steps are avoided. This result evidences the suitability of EC-SOERS for quantitative analysis, as an alternative to EC-SERS.

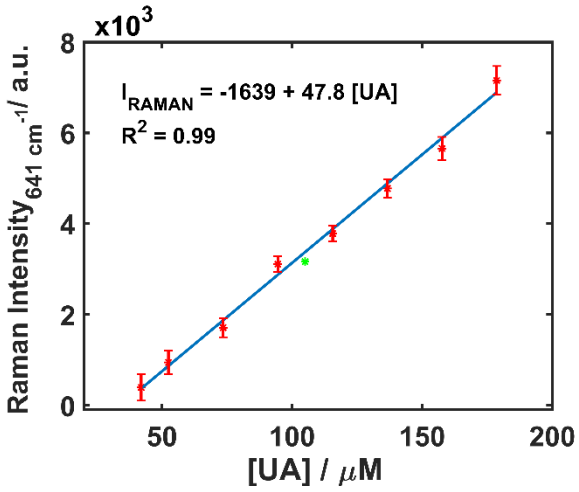

Figure 3. Univariate calibration curve of UA in 0.1 M $HClO_4$ + $5 \cdot 10^{-3}$ M KCl. Raman intensity corresponds to the intensity of the peak at 641 cm^{-1}, at +0.225 V (cd). Red points correspond to the calibration samples, whereas the green point represents the test sample, which has a nominal concentration of 105 µM of UA.

3.4 Quantitative determination of uric acid in synthetic urine using EC-SOERS

Analysis of complex samples represents a big challenge, because matrix effect can be important, provoking for example unexpected baseline modifications in Raman or interferences from compounds present in solution. After demonstrating the usefulness of EC-SOERS for quantitative determination of UA with high reproducibility, the quantification of UA content in a relevant sample was carried out. A sample of synthetic urine containing a nominal concentration of UA was prepared and measured in the same conditions as in the case of the previous section. EC-SOERS depends on Cl^- concentration. Since both, real and synthetic urine have specific Cl^- content, the determination of such content is mandatory in order to adjust the Cl^- concentration needed for the typical EC-SOERS experiment. The adjustment of Cl^- concentration in the sample is simple. To achieve that, a previous calibration curve at different Cl^-

concentration was carried out, by measuring the current intensity in the maximum of the first anodic peak of the cyclic voltammogram. Figure S1 in the supporting information shows the calibration curve for chloride using Ag-SPE electrodes in a solution containing 0.1 M $HClO_4$ and different concentrations of KCl. In this way, the Cl^- content for a sample of synthetic urine was determined.

Usually Cl^- concentration is much higher than $5 \cdot 10^{-3}$ M, and a dilution of the sample is needed to remove the excess of Cl^- and to achieve the desired concentration of Cl^-. For the studied sample, the Cl^- concentration in synthetic urine was determined to be 0.176 M. In consequence, the sample was dilute to obtain $5 \cdot 10^{-3}$ M of Cl^-. Since the test sample is in a relevant and complex matrix, there are some additional problems to determine the UA concentration. In this sense, a first approach was to determine the UA content using a univariate calibration as that previously shown in Figure 2 (see Figure S2 in the supporting information). However, the prediction of the sample yields concentrations of 50.8 and 79.2 µM (with 10.1 % and 44.2 % of error respectively) of UA for two synthetic samples with a nominal UA concentration of 57 and 91 µM respectively.

Traditionally this problem has been solved by using the method of standard addition, as has been demonstrated in previous works [21,53], which can minimize or, in some cases, eliminates completely the matrix effect. This has proven to be an effective method widely used in the literature. However, it presents some disadvantages, for instance: the measurement of each sample requires the preparation of a complete calibration curve, and consequently it is a time-consuming method, requiring long laboratory sessions.

In this work, a much easier and faster way to determine UA concentration in such complex samples is proposed. This method involves the use of PARAFAC [47,48,54] combined with EC-SOERS data to resolve the matrix effect without using the standard addition calibration. An EC-SOERS experiment contains a large number of spectra during a number of potentials, providing a cube of analytical data. A constrained PARAFAC model using the raw data, without any scaling and assuming the non-negativity of the concentrations was constructed. Three components were selected related to the analyte, the baseline and other compounds in solution that can affect to the EC-SOERS process, as will be later explained. To perform the PARAFAC model, a Raman shift range was selected, taking into account the signal coming from the main Raman peaks of the spectra. On the other hand, anodic potentials, where EC-SOERS process is taking place were chosen. Therefore, using all these data should be suitable for extracting the chemical information contained by this cube of data. PARAFAC allows us to separate, from this multivariate spectroscopic response, the UA Raman contribution and, eventually, to obtain the UA concentration with high accuracy. Additionally, the determination of the other components could be possible, as long as the Raman identity of such components were available. On the other hand, PARAFAC could also help to understand the processes taking place along the SEC experiment, as well as the possible interaction between the different components of the sample.

A constrained PARAFAC model assuming the non-negativity of the three factors was applied, which is reasonable because Raman intensities and concentration have to be positive or zero for the applied potentials. As was mentioned above, the main advantage of the PARAFAC model is that the loadings of the UA concentrations can be easily resolved because of the trilinearity of the data. Moreover, the mathematical model is constructed without providing any information about the chemical system, that is to say,

without knowing the nature of the interfering compounds. This model is then compared with the calibration concentrations to assess the UA content of the test sample. It should be highlighted that, if the PARAFAC algorithm converges to the global minimum, which is usual for well-behaved problems, the least-squares solution to the model is found. Three factors were used to resolve the PARAFAC model, which can be further chemically rationalized to the components of the sample. Figure 4A shows the plot of the spectral loadings obtained by PARAFAC as a function of the Raman shift for the three components extracted in the PARAFAC analysis. The three contributions are related with the main components of the sample, namely, UA (orange curve), synthetic urine (yellow curve) and the baseline contribution (blue curve). This is one of the main advantages of using PARAFAC to resolve this system, because avoiding the baseline subtraction not only provides a less time-consuming data treatment but also prevent the addition of variability because of the intrinsic subjective election of the baseline by the operator. In this sense, the separation of the baseline contribution by PARAFAC represents an advantage since provides the possibility of analyzing directly the raw data, without additional tedious pretreatments.

As can be observed, the UA contribution (orange line, Figure 4A) has an identical shape than that for pure UA solution (red line, Figure 1), whereas the baseline contribution follows the behavior of a fluorescence signal in the EC-SOERS measurements when they are carried out with a silver substrate. On the other hand, the yellow curve was ascribed to other components in the synthetic urine since this contribution is potential dependent, and is clearly not present in the pure UA solutions (red line, Figure 1). It is worth noting that, although the identity of all components of synthetic urine is unknown, there is a single clear contribution which can be separated by PARAFAC, probably related to a specific compound present in the matrix that we have not been

able to identify, but that competes with UA to yield an EC-SOERS response (see orange and yellow lines in Figure 4B).

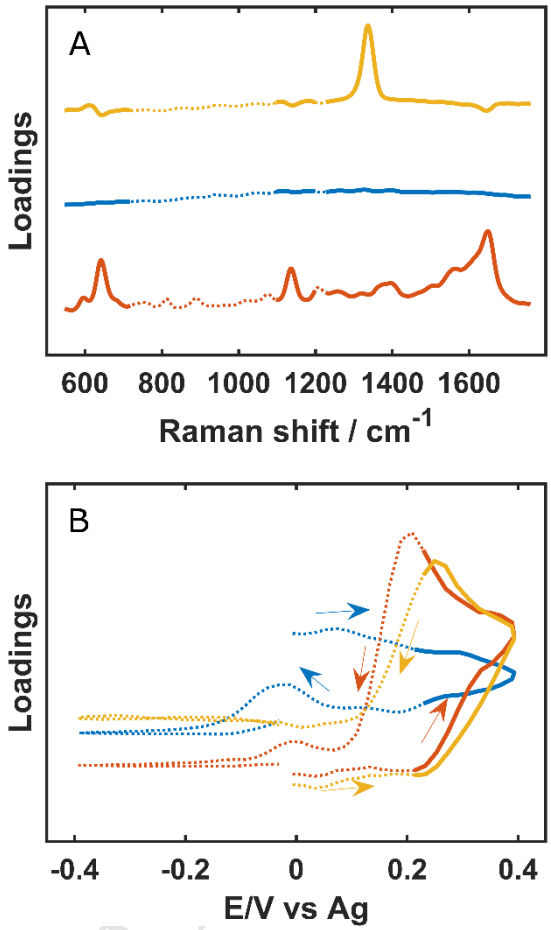

Figure 4. Plot of the loadings, obtained from PARAFAC analysis, as a function of the Raman shift (A) and potential applied (B). The three main components as obtained by PARAFAC analysis correspond to UA (orange line), synthetic urine (yellow line) and the baseline contribution (blue line). Solid lines indicate the zones which are employed to use the PARAFAC model for the prediction of the samples, both in Raman shifts and potentials applied.

Interesting information can be extracted when plotting the loadings obtained by PARAFAC as a function of the applied potential, Figure 4B. In this case, the components related to UA and synthetic urine show a similar enhancement during the electrochemical oxidation of silver (orange and yellow lines, Figure 4B). However, the baseline component has a different behavior, reaching a maximum around a potential of 0.0 V (blue line, Figure 4B). These different behaviors allow PARAFAC to resolve the weight of the contributions as a function of the concentrations, so it can be obtained a calibration curve, similar to that achieved with the univariate data treatment. To build a model that enables the quantification of the UA concentration, only the range of data with a solid line in Figure 4 are introduced in the model in order to remove data that do not contain information about the sample and only introduce noise in the mathematical model. The election of the conditions can be drawn as follow: 1) the inclusion of the main peaks for UA and synthetic urine, corresponded to the regions from 400 to 700 cm^{-1} from 1100 to 1200 cm^{-1} and finally from 1230 to 1670 cm^{-1}; and 2) the potential regions where the changes in the evolution of the loadings *vs* potential are more remarkable, namely, between +0.20 V in the anodic direction and +0.20 V in the cathodic direction.

The model obtained by PARAFAC was robust and allows quantifying UA in relevant samples of synthetic urine. Figure 5 shows the calibration curve plotting the loadings obtained with the PARAFAC model with the UA concentration. As can be observed, the data demonstrate a good linear correlation (R^2=0.99), and acceptable dispersion of the measurements. Using PARAFAC, a concentration of 96 µM was assessed for the test sample with nominal concentration of 91 µM (relative error, 5.5%). The %RSD for this sample was 6.3 %, demonstrating the good reproducibility of the Raman measurements. A limit of detection of 20 µM was obtained. The test sample selected in

the lower limit of the calibration, real concentration 57 µM, was determined with a relative error of 0.2 %, demonstrating that PARAFAC model, in combination with EC-SOERS, provides a fast and easy way to resolve test samples in real complex matrices, using raw data, synthetic calibration samples and avoiding a more complicated method such as standard addition method.

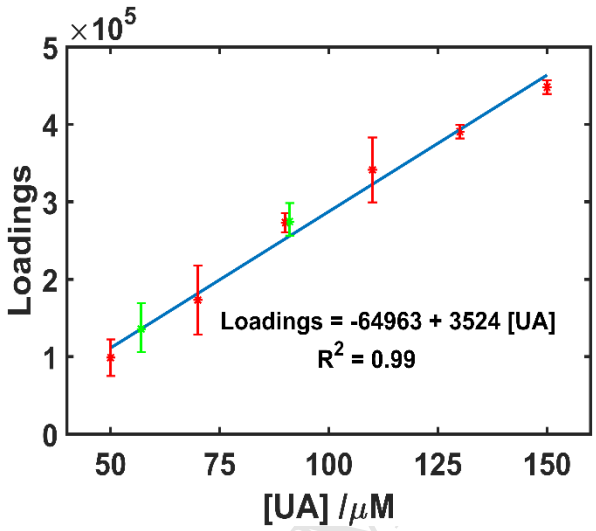

Figure 5. Representation of loadings, obtained from the PARAFAC model, versus concentration of UA. Calibration samples (red) are in a range of concentration of 50 to 150 µM. The test samples (green) have a nominal concentration of 57 and 91 µM.

4. Conclusions

In this work, a new methodology to determine UA in relevant samples is proposed. Such methodology can be used for routine EC-SOERS analysis because of its simplicity and low cost. The use of EC-SOERS has demonstrated to be a good and simple method to generate SOERS substrates that allows the determination of uric acid in synthetic urine with high accuracy and reproducibility. The combination of EC-SOERS with PARAFAC analysis avoids the use of the method of standard addition, which allows the

determination of UA in a complex and relevant matrix with a typical calibration protocol. Additionally, the separation of baseline by PARAFAC eases the use of this technique, eluding previous exhaustive processing of the raw data before the conventional data treatment. Finally, further work need to be done to know if this promising methodology can be used for more real problems both in EC-SOERS and EC-SERS.

ACKNOWLEDGMENTS

Authors acknowledge the financial support from Ministerio de Economía y Competitividad (Grants CTQ2017-83935-R-AEI/FEDERUE) and Junta de Castilla y León (Grant BU297P18). J.V.P-R. thanks JCyL for his postdoctoral fellowship (Grant BU033-U16).

REFERENCES

[1] B. Sharma, R.R. Frontiera, A.I. Henry, E. Ringe, R.P. Van Duyne, SERS: Materials, applications, and the future, Mater. Today. 15 (2012) 16–25. doi:10.1016/S1369-7021(12)70017-2.

[2] S. Schlücker, Surface-Enhanced Raman Spectroscopy: Concepts and Chemical Applications, Angew. Chemie Int. Ed. 53 (2014) 4756–4795. doi:10.1002/anie.201205748.

[3] M. Fleischmann, P.J. Hendra, A.J. McQuillan, Raman spectra of pyridine adsorbed at a silver electrode, Chem. Phys. Lett. 26 (1974) 163–166. doi:10.1016/0009-2614(74)85388-1.

[4] S.S. Nanda, M.J. Kim, K.S. Yeom, S.S.A. An, H. Ju, D.K. Yi, Raman spectrum

of graphene with its versatile future perspectives, TrAC - Trends Anal. Chem. 80 (2016) 125–131. doi:10.1016/j.trac.2016.02.024.

[5] J. Depciuch, E. Kaznowska, I. Zawlik, R. Wojnarowska, M. Cholewa, P. Heraud, J. Cebulski, Application of Raman Spectroscopy and Infrared Spectroscopy in the Identification of Breast Cancer, Appl. Spectrosc. 70 (2016) 251–263. doi:10.1177/0003702815620127.

[6] Z. Li, J. Wang, D. Li, Applications of Raman spectroscopy in detection of water quality, Appl. Spectrosc. Rev. 51 (2016) 313–337. doi:10.1080/05704928.2015.1131711.

[7] P.L. Stiles, J.A. Dieringer, N.C. Shah, R.P. Van Duyne, Surface-Enhanced Raman Spectroscopy, Annu. Rev. Anal. Chem. 1 (2008) 601–626. doi:10.1146/annurev.anchem.1.031207.112814.

[8] S.Y. Ding, E.M. You, Z.Q. Tian, M. Moskovits, Electromagnetic theories of surface-enhanced Raman spectroscopy, Chem. Soc. Rev. 46 (2017) 4042–4076. doi:10.1039/c7cs00238f.

[9] D.Y. Wu, X.M. Liu, S. Duan, X. Xu, B. Ren, S.H. Lin, Z.Q. Tian, Chemical enhancement effects in SERS spectra: A quantum chemical study of pyridine interacting with copper, silver, gold and platinum metals, J. Phys. Chem. C. 112 (2008) 4195–4204. doi:10.1021/jp0760962.

[10] M. Moskovits, Surface-enhanced spectroscopy, Rev. Mod. Phys. 57 (1985) 783–826. doi:10.1103/RevModPhys.57.783.

[11] X.-M. Lin, Y. Cui, Y.-H. Xu, B. Ren, Z.-Q. Tian, Surface-enhanced Raman spectroscopy: substrate-related issues, Anal. Bioanal. Chem. 394 (2009) 1729–

1745. doi:10.1007/s00216-009-2761-5.

[12] D.-Y. Wu, J.-F. Li, B. Ren, Z. Tian, Electrochemical surface-enhanced Raman spectroscopy of nanostructures, Chem. Soc. Rev. 37 (2008) 1025–1041. doi:10.1039/b707872m.

[13] Z.-Q. Tian, B. Ren, Adsorption and Reaction at Electrochemical Interfaces as Probed by Surface-Enhanced Raman Spectroscopy, Annu. Rev. Phys. Chem. 55 (2004) 197–229. doi:10.1146/annurev.physchem.54.011002.103833.

[14] J.H. Zhong, J.Y. Liu, Q. Li, M.G. Li, Z.C. Zeng, S. Hu, D.Y. Wu, W. Cai, B. Ren, Interfacial capacitance of graphene: Correlated differential capacitance and in situ electrochemical Raman spectroscopy study, Electrochim. Acta. 110 (2013) 754–761. doi:10.1016/j.electacta.2013.04.004.

[15] G. Agrawal, S.K. Samal, Raman Spectroscopy for Advanced Polymeric Biomaterials, ACS Biomater. Sci. Eng. 4 (2018) 1285–1299. doi:10.1021/acsbiomaterials.8b00258.

[16] D. Ibañez, A. Santidrian, A. Heras, M. Kalbáč, A. Colina, Study of Adenine and Guanine Oxidation Mechanism by Surface-Enhanced Raman Spectroelectrochemistry, J. Phys. Chem. C. 119 (2015) 8191–8198. doi:10.1021/acs.jpcc.5b00938.

[17] D. Martín-Yerga, A. Pérez-Junquera, M.B. González-García, J. V. Perales-Rondon, A. Heras, A. Colina, D. Hernández-Santos, P. Fanjul-Bolado, Quantitative Raman spectroelectrochemistry using silver screen-printed electrodes, Electrochim. Acta. 264 (2018) 183–190. doi:10.1016/j.electacta.2018.01.060.

[18] B.H.C. Greene, D.S. Alhatab, C.C. Pye, C.L. Brosseau, Electrochemical-Surface Enhanced Raman Spectroscopic (EC-SERS) Study of 6-Thiouric Acid: A Metabolite of the Chemotherapy Drug Azathioprine, J. Phys. Chem. C. 121 (2017) 8084–8090. doi:10.1021/acs.jpcc.7b01179.

[19] L. Zhao, J. Blackburn, C.L. Brosseau, Quantitative Detection of Uric Acid by Electrochemical-Surface Enhanced Raman Spectroscopy Using a Multilayered Au/Ag Substrate, Anal. Chem. 87 (2015) 441–447. doi:10.1021/ac503967s.

[20] A.M. Robinson, S.G. Harroun, J. Bergman, C.L. Brosseau, Portable Electrochemical Surface-Enhanced Raman Spectroscopy System for Routine Spectroelectrochemical Analysis, Anal. Chem. 84 (2012) 1760–1764. doi:10.1021/ac2030078.

[21] C. Westley, Y. Xu, B. Thilaganathan, A.J. Carnell, N.J. Turner, R. Goodacre, Absolute Quantification of Uric Acid in Human Urine Using Surface Enhanced Raman Scattering with the Standard Addition Method, Anal. Chem. 89 (2017) 2472–2477. doi:10.1021/acs.analchem.6b04588.

[22] K.L. Norrod, L.M. Sudnik, D. Rousell, K.L. Rowlen, Quantitative Comparison of Five SERS Substrates: Sensitivity and Limit of Detection, Appl. Spectrosc. 51 (1997) 994–1001. doi:10.1366/0003702971941377.

[23] X. Han, H. Wang, X. Ou, X. Zhang, Highly sensitive, reproducible, and stable SERS sensors based on well-controlled silver nanoparticle-decorated silicon nanowire building blocks, J. Mater. Chem. 22 (2012) 14127–14132. doi:10.1039/c2jm31443f.

[24] R. Goodacre, D. Graham, K. Faulds, Recent developments in quantitative SERS:

Moving towards absolute quantification, TrAC - Trends Anal. Chem. 102 (2018) 359–368. doi:10.1016/j.trac.2018.03.005.

[25] K. Hering, D. Cialla, K. Ackermann, T. Dörfer, R. Möller, H. Schneidewind, R. Mattheis, W. Fritzsche, P. Rösch, J. Popp, SERS: A versatile tool in chemical and biochemical diagnostics, Anal. Bioanal. Chem. 390 (2008) 113–124. doi:10.1007/s00216-007-1667-3.

[26] J. V. Perales-Rondon, S. Hernandez, D. Martin-Yerga, P. Fanjul-Bolado, A. Heras, A. Colina, Electrochemical surface oxidation enhanced Raman scattering, Electrochim. Acta. 282 (2018) 377–383. doi:10.1016/j.electacta.2018.06.079.

[27] R.C. Trivedi, L. Rebar, E. Berta, L. Stong, New enzymatic method for serum uric acid at 500 nm., Clin. Chem. 24 (1978) 1908–1911. http://www.ncbi.nlm.nih.gov/pubmed/709818.

[28] X. Wang, F. Li, Z. Cai, K. Liu, J. Li, B. Zhang, J. He, Sensitive colorimetric assay for uric acid and glucose detection based on multilayer-modified paper with smartphone as signal readout, Anal. Bioanal. Chem. 410 (2018) 2647–2655. doi:10.1007/s00216-018-0939-4.

[29] E.F.M. Gabriel, P.T. Garcia, T.M.G. Cardoso, F.M. Lopes, F.T. Martins, W.K.T. Coltro, Highly sensitive colorimetric detection of glucose and uric acid in biological fluids using chitosan-modified paper microfluidic devices, Analyst. 141 (2016) 4749–4756. doi:10.1039/C6AN00430J.

[30] W.D. Slaunwhite, L.A. Pachla, D.C. Wenke, P.T. Kissinger, Colorimetric, enzymatic, and liquid-chromatographic methods for serum uric acid compared., Clin. Chem. 21 (1975) 1427–1429.

http://www.ncbi.nlm.nih.gov/pubmed/1157308.

[31] K. Honeychurch, The Determination of Uric Acid in Human Saliva by Liquid Chromatography with Electrochemical Detection, J. Anal. Bioanal. Sep. Tech. 2 (2017) 47–51. doi:10.15436/2476-1869.17.1280.

[32] J. E. Young, J. J. Pesek, M. T. Matyska, B. Sanchez, B. White, Quantitative Analysis of Uric Acid Metabolites in Urine by High Performance Liquid Chromatography - Mass Spectrometry Using Silica Hydride Columns, Curr. Chromatogr. 4 (2017) 51–57. doi:10.2174/2213240604666170106160806.

[33] Y. Zuo, Y. Yang, Z. Zhu, W. He, Z. Aydin, Determination of uric acid and creatinine in human urine using hydrophilic interaction chromatography, Talanta. 83 (2011) 1707–1710. doi:10.1016/j.talanta.2010.11.073.

[34] Riyanto, I. Rofida, Preparation and application of nickel plating on copper electrode (NPCE) for uric acid analysis in human urine using cyclic voltammetry, Int. J. Electrochem. Sci. 14 (2019) 2290–2304. doi:10.20964/2019.03.35.

[35] M. Govindasamy, V. Mani, S.M. Chen, A. Sathiyan, J.P. Merlin, V.K. Ponnusamy, Sensitive and selective determination of uric acid using polyaniline and iron composite film modified electrode, Int. J. Electrochem. Sci. 11 (2016) 8730–8737. doi:10.20964/2016.10.63.

[36] L.L. Qu, Q. Jia, C. Liu, W. Wang, L. Duan, G. Yang, C.Q. Han, H. Li, Thin layer chromatography combined with surface-enhanced raman spectroscopy for rapid sensing aflatoxins, J. Chromatogr. A. 1579 (2018) 115–120. doi:10.1016/j.chroma.2018.10.024.

[37] O. Durucan, K. Wu, M. Viehrig, T. Rindzevicius, A. Boisen, Nanopillar-Assisted

SERS Chromatography, ACS Sensors. 3 (2018) 2492–2498. doi:10.1021/acssensors.8b00887.

[38] G. Trachta, B. Schwarze, B. Sägmüller, G. Brehm, S. Schneider, Combination of high-performance liquid chromatography and SERS detection applied to the analysis of drugs in human blood and urine, J. Mol. Struct. 693 (2004) 175–185. doi:10.1016/j.molstruc.2004.02.034.

[39] A. Tycova, J. Prikryl, F. Foret, Recent strategies toward microfluidic-based surface-enhanced Raman spectroscopy, Electrophoresis. 38 (2017) 1977–1987. doi:10.1002/elps.201700046.

[40] L. Chen, J. Choo, Recent advances in surface-enhanced Raman scattering detection technology for microfluidic chips, Electrophoresis. 29 (2008) 1815–1828. doi:10.1002/elps.200700554.

[41] A. Tycova, R.F. Gerhardt, D. Belder, Surface enhanced Raman spectroscopy in microchip electrophoresis, J. Chromatogr. A. 1541 (2018) 39–46. doi:10.1016/j.chroma.2018.02.014.

[42] E. Kämmer, K. Olschewski, S. Stöckel, P. Rösch, K. Weber, D. Cialla-May, T. Bocklitz, J. Popp, Quantitative SERS studies by combining LOC-SERS with the standard addition method, Anal. Bioanal. Chem. 407 (2015) 8925–8929. doi:10.1007/s00216-015-9045-z.

[43] I.J. Hidi, M. Jahn, K. Weber, T. Bocklitz, M.W. Pletz, D. Cialla-May, J. Popp, Lab-on-a-Chip-Surface Enhanced Raman Scattering Combined with the Standard Addition Method: Toward the Quantification of Nitroxoline in Spiked Human Urine Samples, Anal. Chem. 88 (2016) 9173–9180.

doi:10.1021/acs.analchem.6b02316.

[44] C.M. Andersen, R. Bro, Practical aspects of PARAFAC modeling of fluorescence excitation-emission data, J. Chemom. 17 (2003) 200–215. doi:10.1002/cem.790.

[45] N. González-Diéguez, A. Colina, J. López-Palacios, A. Heras, Spectroelectrochemistry at Screen-Printed Electrodes: Determination of Dopamine, Anal. Chem. 84 (2012) 9146–9153. doi:10.1021/ac3018444.

[46] J. Garoz-Ruiz, C. Guillen-Posteguillo, A. Colina, A. Heras, Application of spectroelectroanalysis for the quantitative determination of mixtures of compounds with highly overlapping signals, Talanta. 195 (2019) 815–821. doi:10.1016/j.talanta.2018.12.002.

[47] R. Bro, PARAFAC. Tutorial and applications, Chemom. Intell. Lab. Syst. 38 (1997) 149–171. doi:10.1016/S0169-7439(97)00032-4.

[48] A. Muñoz de la Peña, A. Espinosa Mansilla, D. González Gómez, A.C. Olivieri, H.C. Goicoechea, Interference-free analysis using three-way fluorescence data and the parallel factor model. Determination of fluoroquinolone antibiotics in human serum, Anal. Chem. 75 (2003) 2640–2646. doi:10.1021/ac026360h.

[49] C. a Andersson, R. Bro, The N-way Toolbox for MATLAB, Chemom. Intell. Lab. Syst. 52 (2000) 1–4. doi:10.1016/S0169-7439(00)00071-X.

[50] J. Cabalo, J.A. Guicheteau, S. Christesen, Toward understanding the influence of intermolecular interactions and molecular orientation on the chemical enhancement of SERS, J. Phys. Chem. A. 117 (2013) 9028–9038. doi:10.1021/jp403458k.

[51] Y. Fleger, Y. Mastai, M. Rosenbluh, D.H. Dressler, SERS as a probe for adsorbate orientation on silver nanoclusters, J. Raman Spectrosc. 40 (2009) 1572–1577. doi:10.1002/jrs.2300.

[52] J. V. Perales-Rondon, S. Hernandez, A. Heras, A. Colina, Effect of chloride and pH on the electrochemical surface oxidation enhanced Raman scattering, Appl. Surf. Sci. 473 (2019) 366–372. doi:10.1016/j.apsusc.2018.12.148.

[53] J.E.L. Villa, R.J. Poppi, A portable SERS method for the determination of uric acid using a paper-based substrate and multivariate curve resolution, Analyst. 141 (2016) 1966–1972. doi:10.1039/c5an02398j.

[54] K.S. Booksh, B.R. Kowalski, Theory of Analytical Chemistry, Anal. Chem. 66 (1994) 782–791. doi:10.1021/ac00087a001.

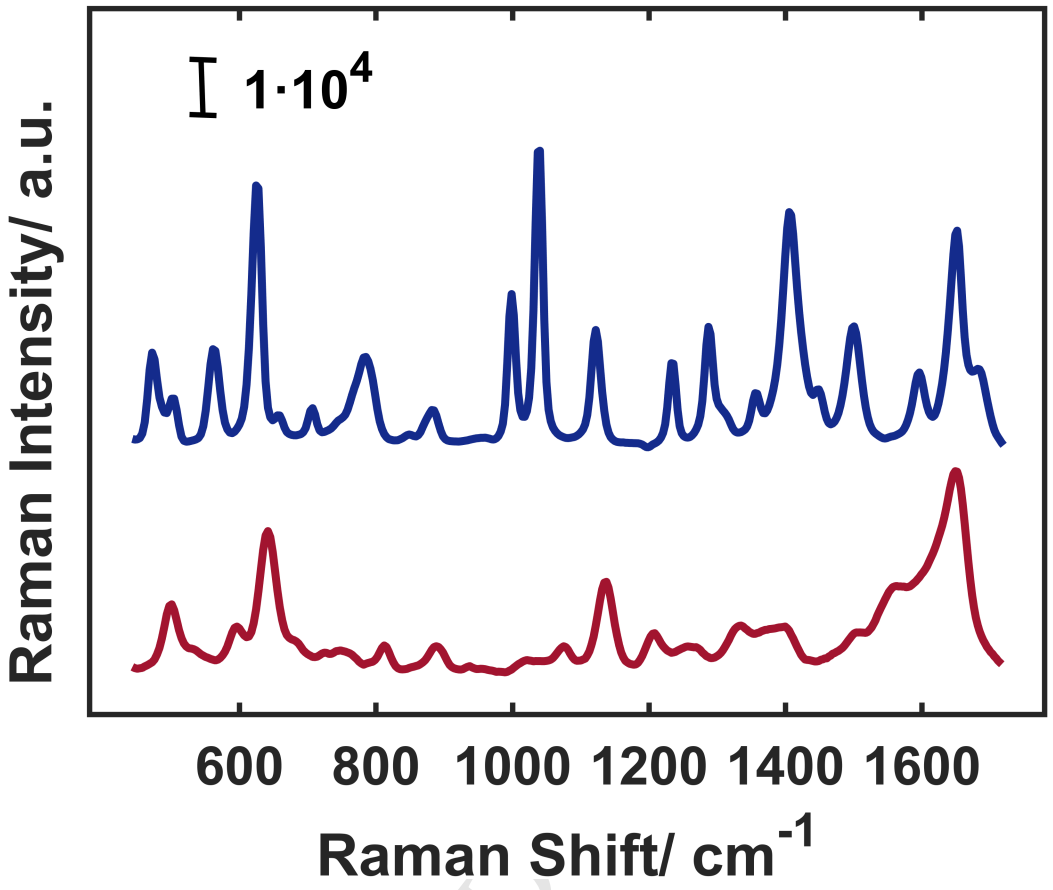
1·10^4
Raman Intensity/ a.u.
600
800
1000
1200
1400
1600
Raman Shift/ cm^-1

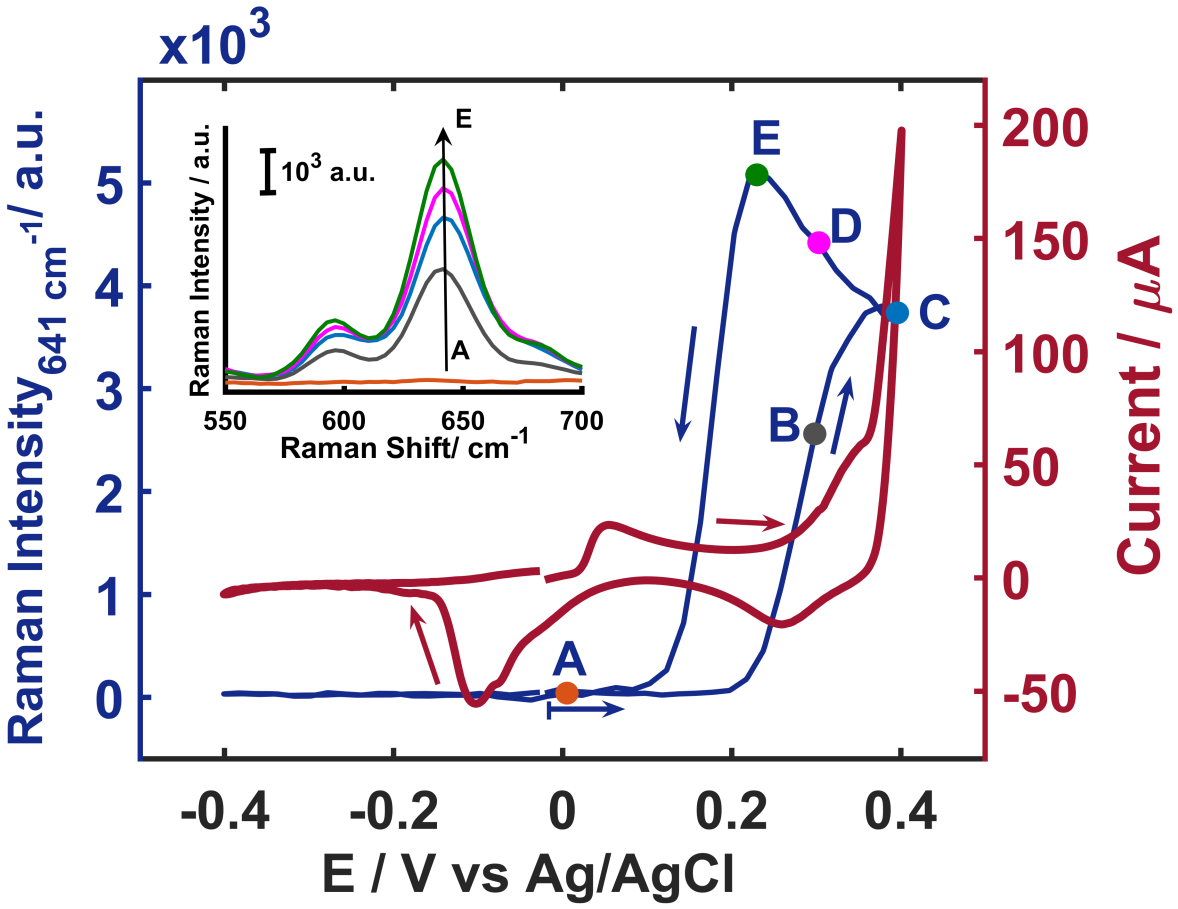
x10^3
Raman Intensity641 cm-1/ a.u.
Current / μA
E / V vs Ag/AgCl
Raman Intensity / a.u.
10^3 a.u.
Raman Shift/ cm-1
A
B
C
D
E

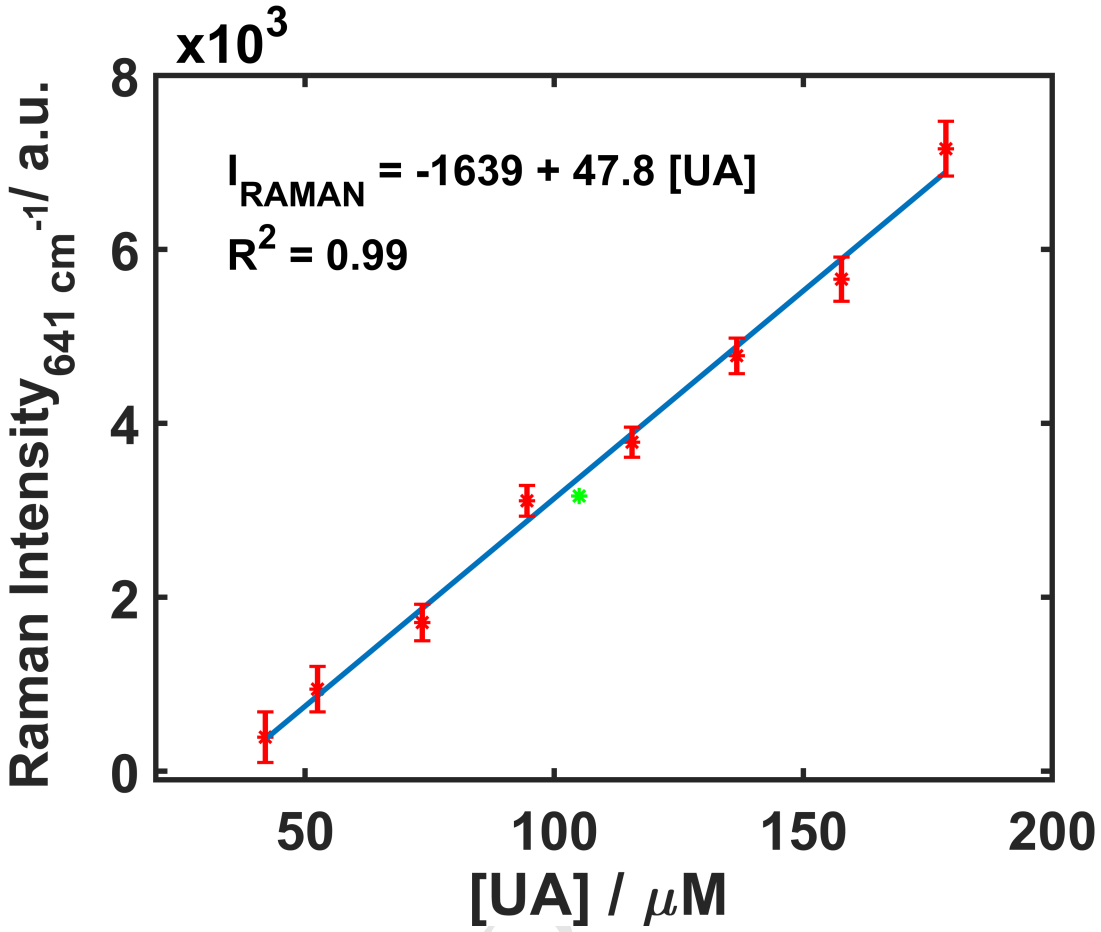
x10^3
8
6
4
2
0
Raman Intensity641 cm-1/ a.u.
I RAMAN = -1639 + 47.8 [UA]
R2 = 0.99
50
100
150
200
[UA] / μM

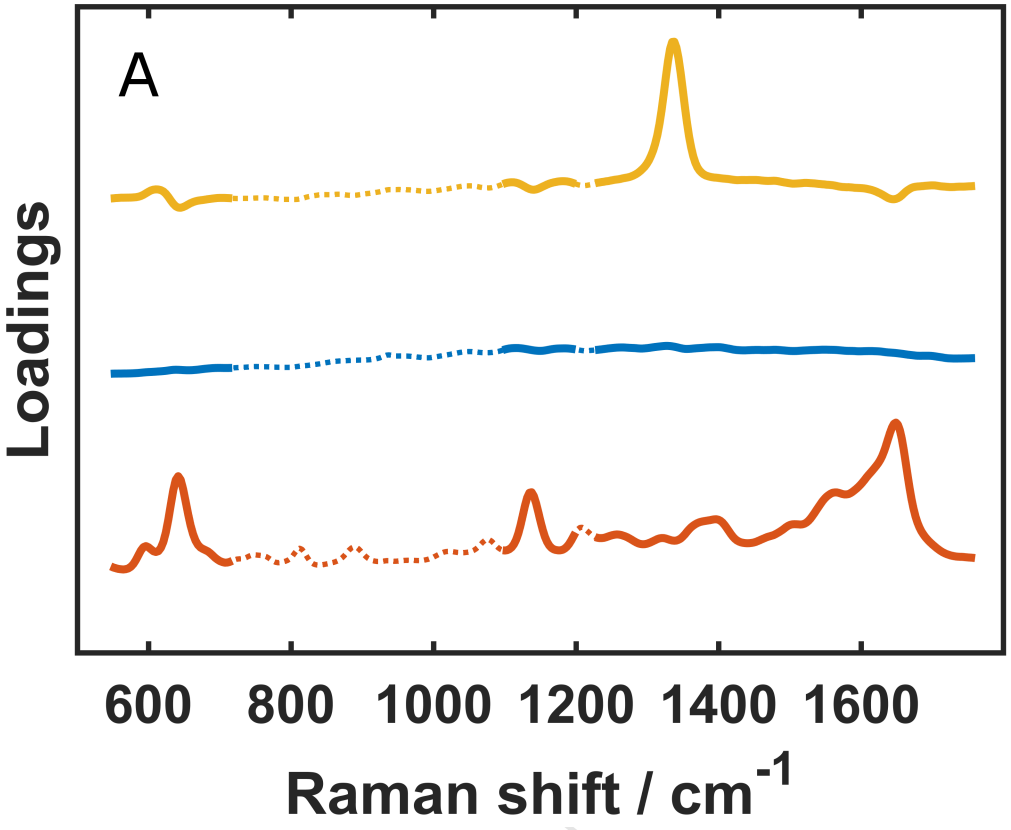

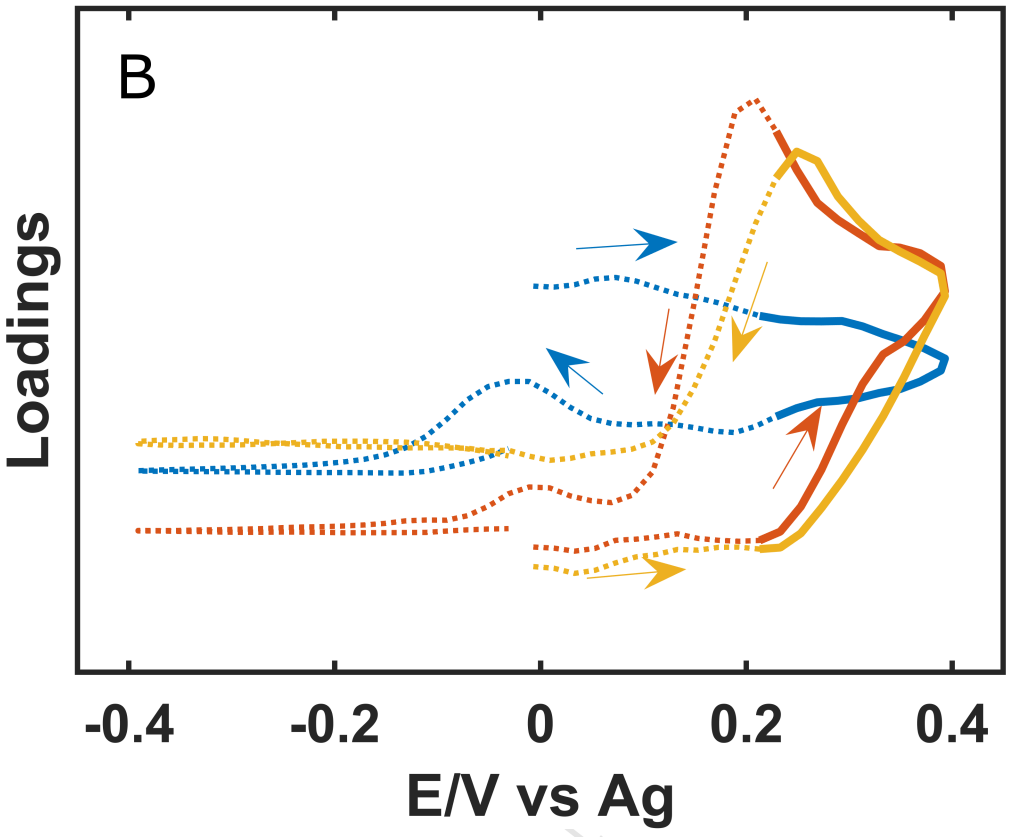

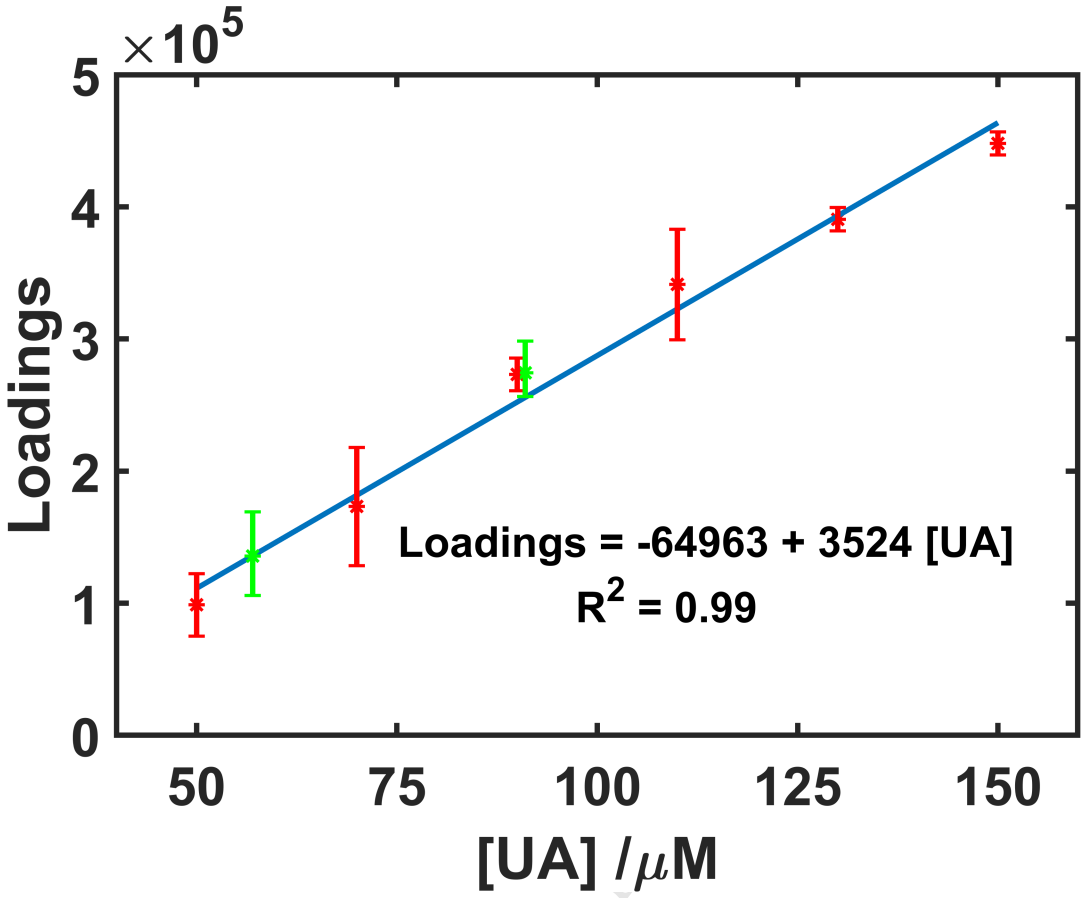

- EC-SOERS has been used in a complex medium
- Uric acid has been determined in synthetic urine using simple calibration standards
- No baseline correction has been used to quantify uric acid with the evolution of the Raman signal
- Raman spectroelectrochemical trinilinear data facilitate the quantification

Declaration of interests

☒ The authors declare that they have no known competing financial interests or personal relationships that could have appeared to influence the work reported in this paper.

☐The authors declare the following financial interests/personal relationships which may be considered as potential competing interests: